A systematic study of Galactic infrared bubbles along the whole Galactic plane with the *AKARI* all-sky surveys

Misaki Hanaoka,[1] Hidehiro Kaneda,[1] Toyoaki Suzuki,[1] Takuma Kokusho,[1] Shinki Oyabu,[1] and Daisuke Ishihara[1]

[1]*Graduate School of Science, Nagoya University, Furo-cho, Chikusa-ku, Nagoya 464-8602, Japan*

ABSTRACT

Galactic infrared (IR) bubbles are known to contain massive stars near their centers, and crucial to study massive star formation mechanisms. In our previous study (Hattori et al. 2016), IR bubbles located in inner Galactic regions ($|l| \leq 65°$, $|b| \leq 1°$) are classified into broken and closed bubbles, depending on their morphologies, to find that the broken bubbles are indicative of cloud-cloud collision. We expand the previous study to the whole Galactic plane using the *AKARI* all-sky survey data. We limit our study on large ($R > 1'$) bubbles to reliably identify and classify them even in outer Galactic regions and relatively high-latitude regions where neither *Spitzer* nor *Herschel* data are available. As a result, we newly discover about 100 Galactic IR bubbles in outer Galactic regions ($|l| > 65°$, $|b| \leq 5°$). We find that a significantly higher fraction of bubbles are classified into broken ones in outer Galactic regions than in inner Galactic regions. Following the same procedure as in Hattori et al. (2016), we also examine the properties of the bubbles, decomposing their spectral energy distributions consisting of *AKARI* and *Herschel* photometric data with a dust model. In the paper, we show the result of our comparative study on the properties of the Galactic IR bubbles between the inner and outer Galactic regions, and discuss the cause of their systematic difference.

Keywords: Bubbles, Milky Way, Massive star formation, ISM, Dust extinction

1. INTRODUCTION

There are a lot of Galactic infrared (IR) bubbles along the Galactic plane. They have shell-like structures which are clearly seen in the polycyclic aromatic hydrocarbon (PAH) emission. The IR bubbles are thought to be formed by UV radiation from central massive stars. Churchwell et al. (2006, 2007) found about 600 bubbles in inner Galactic regions ($|l| \leq 65°$, $|b| \leq 1°$) using the 8 μm band images of the Galactic Legacy Infrared Mid-plane Survey Extraordinaire (GLIMPSE: Benjamin et al. 2003; Churchwell et al. 2009) program with *Spitzer*. They created a catalog and classified the IR bubbles into two categories, broken and closed bubbles, by their visual morphologies.

Hattori et al. (2016) obtained the central position and shell radius of each object and established the quantitative criteria for classification of the shell morphologies. In addition, they derived the IR luminosity of each bubble using 6 images in the 9, 18, 65, 90, 140 and 160 μm bands of the *AKARI* all-sky survey data. They found a tight correlation between the total IR luminosity and the shell radius, which follows the conventional picture of the Strömgrem sphere. Then, they discussed the massive star formation mechanisms based on the following results: large broken bubbles have higher total IR luminosities, lower fractional luminosities of the PAH emission and dust heating sources located nearer to the shells. Finally, they concluded that these large broken bubbles are likely to be formed by cloud-cloud collision (CCC) mechanism.

The previous study investigated IR bubbles in inner Galactic regions. However, there are a number of IR bubbles in outer Galactic regions which have never been listed. We expand the previous study to the whole Galactic plane using the *AKARI* all-sky survey data. We obtain the morphologies and the IR luminosities of the IR bubbles in outer Galactic regions. To improve the estimation of the IR luminosity, we also add far-IR and submillimeter wavelength fluxes using the *Herschel* infrared Galactic plane survey (Hi-GAL: Molinari et al. 2010; Molinari et al. 2016) data. Then, we compare the properties of IR bubbles in outer Galactic regions with those in inner Galactic regions. From the results, we discuss the differences of environments and star-formation mechanisms between IR bubbles in inner and outer Galactic regions.

Corresponding author: Misaki Hanaoka
hanaoka@u.phys.nagoya-u.ac.jp

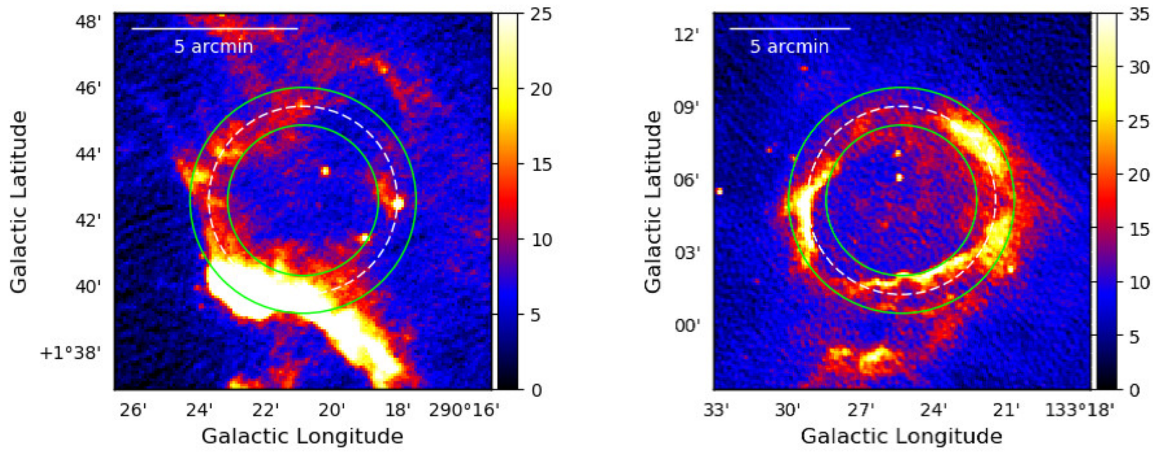

Figure 1. Examples of the *AKARI* 9 μm band images of the IR bubbles newly found in this study. The left panel shows a broken bubble, while the right panel shows a closed bubble. The white dashed line shows the radius of the bubble, while the green annulus is the shell region defined in this study.

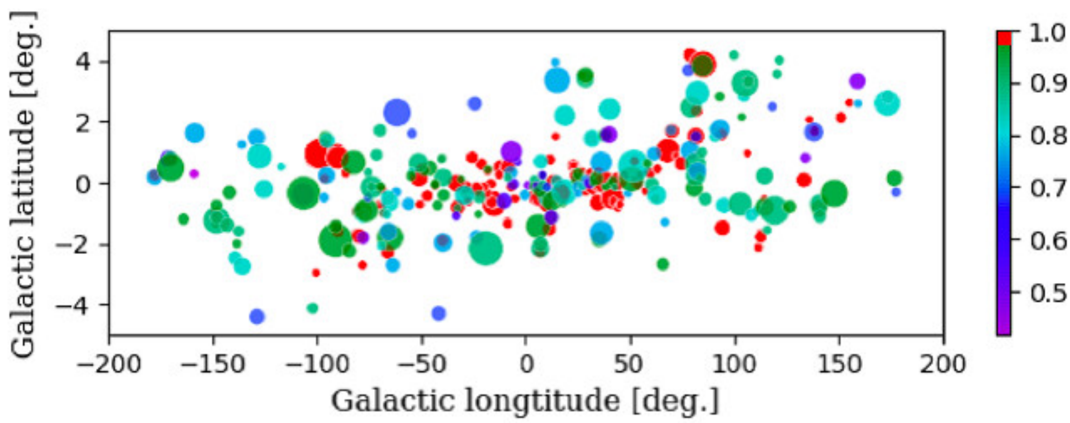

Figure 2. Positions of the IR bubbles. The symbol size shows the angular radius of each bubble, while the color bar shows the covering fraction of the shell morphology.

2. OBSERVATION AND DATA ANALYSIS

In this study, we investigate high-latitude inner Galactic regions ($|l| \leq 65°$, $1° < |b| \leq 5°$) and outer Galactic regions ($|l| > 65°$, $|b| \leq 5°$). We newly found 180 IR bubbles which consist of 38 objects in high-latitude inner Galactic regions and 142 objects in outer Galactic regions (Figure 1). Note that we limit our study on large ($R > 1'$) bubbles to reliably identify them. We obtained the center position and the shell radius of each IR bubble, following the same procedure as in Hattori et al. (2016). We derived the covering fraction of each IR bubble. To evaluate the IR bubbles of various sizes and brightness in an unbiased manner, we divided the annular shell into 12 sectors equally and judged whether each sector is opened or filled by the classification criteria established by Hattori et al. (2016).

Moreover, we estimated the IR luminosity by creating the spectral energy distribution (SED) of each IR bubble. We used the *AKARI* all-sky survey data (9, 18, 65, 90, 140 μm bands images) and *Herschel* Hi-GAL data (70, 160, 250, 350, 500 μm) to derive the flux densities. In high-latitude regions ($1° < |b| \leq 5°$) where there is no *Herschel* Hi-GAL data, we used only 6 bands images of the *AKARI* all-sky survey data (9, 18, 65, 90, 140 and 160 μm). The photometry aperture is defined as $< 2\,R$ annular region centered at (l, b) of each bubble.To obtain the total IR luminosities and decompose them to dust components, we fit the SEDs by a dust model composed of PAHs (Draine & Li 2007), warm dust and cold dust.

3. RESULT

Figure 2 shows the positions and the covering fractions of the IR bubbles including the objects cataloged in Churchwell et al. (2006, 2007). The figure indicates that the covering fractions of the IR bubbles in outer Galactic regions are lower than those in inner Galactic regions. Moreover, these IR bubbles in outer Galactic regions have larger angular radii. Hence bubbles in outer Galactic regions tend to exhibit large broken morphologies.

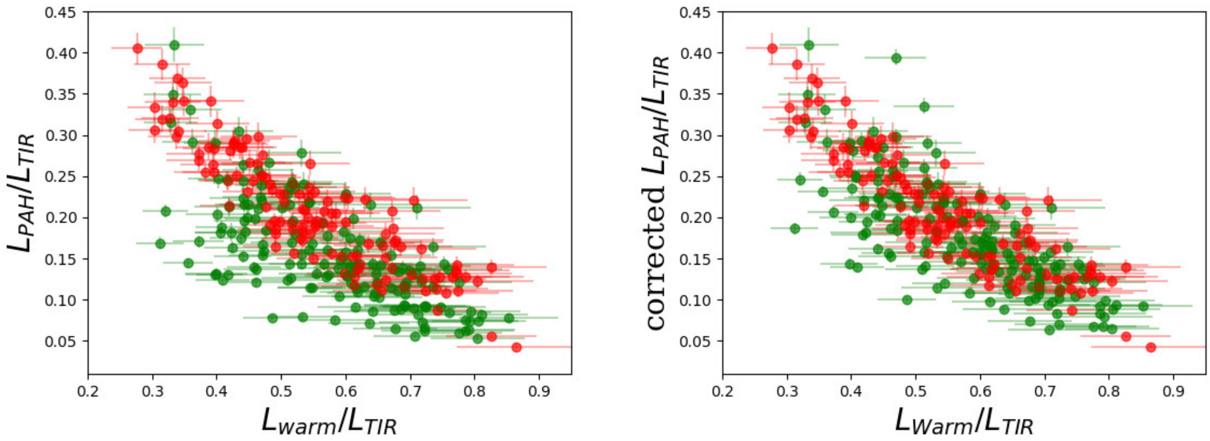

Figure 3. Left panel shows the relationship between $L_{\mathrm{PAH}}/L_{\mathrm{TIR}}$ and $L_{\mathrm{warm}}/L_{\mathrm{TIR}}$. The red and green points correspond to the data points of the IR bubbles in inner and outer Galactic regions, respectively. The right panel is the same as the left panel, but the effect of dust extinction is taken into account.

Based on the result of the SED fitting, we also investigate the relationship of the luminosity ratios, $L_{\mathrm{PAH}}/L_{\mathrm{TIR}}$ and $L_{\mathrm{warm}}/L_{\mathrm{TIR}}$. Figure 3 shows that there is a significant anti-correlation between $L_{\mathrm{PAH}}/L_{\mathrm{TIR}}$ and $L_{\mathrm{warm}}/L_{\mathrm{TIR}}$. Moreover this study suggests a systematic difference in the relationship between inner and outer Galactic regions.

4. DISCUSSION

First, we discuss the result of the bubble morphology and distribution. From Figure 2, we find that IR bubbles in outer Galactic regions have lower covering fractions and larger angular radii. If these IR bubbles are formed by CCC, the shell structures are likely to be broken and the massive stars may be located near the edge of the shell, because of the compressed gas on the collision surface (Habe & Ohta 1992). Hattori et al. (2016) suggested that the massive stars in large broken bubbles are likely to be formed by CCC. Then, our result implies that CCC might be a dominant process of massive star formation in outer Galactic regions. We need to verify this possibility by investigating the positions of massive stars and PAH fractional luminosities as a shock tracer in future.

The left panel of Figure 3 shows a negative correlation between $L_{\mathrm{PAH}}/L_{\mathrm{TIR}}$ and $L_{\mathrm{warm}}/L_{\mathrm{TIR}}$. The negative correlation can be explained by strong UV radiation from massive star, because the strong radiation is expected to increase $L_{\mathrm{warm}}/L_{\mathrm{TIR}}$ and photodissociate PAHs (i.e., decrease $L_{\mathrm{PAH}}/L_{\mathrm{TIR}}$). The left panel in Figure 3 also indicates difference in the relationship between the inner and outer Galactic regions. In order to estimate the effect of interstellar dust extinction on the difference, we assume a systematic difference in the hydrogen gas density by $\Delta n_{\mathrm{H}} = 1\ \mathrm{cm}^{-3}$ between the inner and outer Galactic regions, so that the extinction may attenuate L_{PAH} of the bubbles in inner Galactic regions with the following optical depth:

$$\tau = C_{\mathrm{ext}}\, \Delta n_{\mathrm{H}}\, l, \tag{1}$$

where l is the distance to each bubble and C_{ext} is the cross section of the interstellar dust extinction. In our calculation, we used C_{ext} at wavelength 7.7 μm, $C_{\mathrm{ext}} = 1.1 \times 10^{-23}\ \mathrm{cm}^2$ (Weingartner & Draine 2001; Draine & Li 2007). The right panel in Figure 3 shows the relationship thus corrected for the dust extinction. The figure suggests that the systematic difference may not be able to be explained by the extinction alone. Moreover, many of the bubbles with low $L_{\mathrm{warm}}/L_{\mathrm{TIR}}$ have unusually high $L_{\mathrm{PAH}}/L_{\mathrm{TIR}}$. Smith et al. (2007) showed that the typical value of $L_{\mathrm{PAH}}/L_{\mathrm{TIR}}$ is about 10% and extended up to 20% in star-forming galaxies. We will discuss the implications of this result in a separate paper.

5. CONCLUSION

We have investigated Galactic IR bubbles along the whole Galactic plane using the *AKARI* all-sky survey data. We have newly found 180 IR bubbles which consist of 38 objects in high-latitude inner Galactic regions ($|l| \leq 65°$, $1° < |b| \leq 5°$) and 142 objects in outer Galactic regions ($|l| > 65°$, $|b| \leq 5°$). We derived the covering fractions of each IR bubble and also estimated the IR fluxes using the *AKARI* all-sky survey and *Herschel* Hi-GAL data.

From our results, we find that the IR bubbles in outer Galactic regions have lower covering fractions and larger angular radii. Hattori et al. (2016) suggested that the massive stars in the large broken bubbles are likely to be formed by cloud-cloud collision process. Thus, our result implies that cloud-cloud collision might be a dominant star formation process in outer Galactic regions. Moreover, we find that a negative correlation between $L_{\mathrm{warm}}/L_{\mathrm{TIR}}$ and $L_{\mathrm{PAH}}/L_{\mathrm{TIR}}$. The negative correlation can be explained by strong UV radiation from massive star, because the strong radiation is expected to increase $L_{\rm warm}/L_{\rm TIR}$ and photodissociate PAHs (i.e., decrease $L_{\rm PAH}/L_{\rm TIR}$). We also find that many of the bubbles with low $L_{\rm warm}/L_{\rm TIR}$ have unusually high $L_{\rm PAH}/L_{\rm TIR}$.

REFERENCES

Benjamin, R. A., Churchwell, E., Babler, B. L., et al. 2003, PASP, 115, 953
Churchwell, E., Povich, M. S., Allen, D., et al. 2006, ApJ, 649, 759
Churchwell, E., Watson, D. F., Povich, M. S., et al. 2007, ApJ, 670, 428
Churchwell, E., Babler, B. L., Meade, M. R., et al. 2009, PASP, 121, 213
Draine, B. T., & Li, A. 2007, ApJ, 657, 810
Habe, A., & Ohta, K. 1992, PASJ, 44, 203
Hattori, Y., Kaneda, H., Ishihara, D., et al. 2016, PASJ, 68, 37
Molinari, S., Schisano, E., Elia, D., et al. 2016, A&A, 591, A149
Molinari, S., Swinyard, B., Bally, J., et al. 2010, A&A, 518, L100
Smith, J. D. T., Draine, B. T., Dale, D. A., et al. 2007, ApJ, 656, 770
Weingartner, J. C., & Draine, B. T. 2001, ApJ, 548, 296